small
NANO MICRO

Nanohybrids

Electronic Interactions between "Pea" and "Pod": The Case of Oligothiophenes Encapsulated in Carbon Nanotubes

Jia Gao, Pascal Blondeau, Patrizio Salice, Enzo Menna, Barbora Bártová, Cécile Hébert,* Jens Leschner, Ute Kaiser, Matus Milko, Claudia Ambrosch-Draxl,* and Maria Antonietta Loi**

One of the most challenging strategies to achieve tunable nanophotonic devices is to build robust nanohybrids with variable emission in the visible spectral range, while keeping the merits of pristine single-walled carbon nanotubes (SWNTs). This goal is realized by filling SWNTs ("pods") with a series of oligothiophene molecules ("peas"). The physical properties of these peapods are depicted by using aberration-corrected high-resolution transmission electron microscopy, Raman spectroscopy, and other optical methods including steady-state and time-resolved measurements. Visible photoluminescence with quantum yields up to 30% is observed for all the hybrids. The underlying electronic structure is investigated by density functional theory calculations for a series of peapods with different molecular lengths and tube diameters, which demonstrate that van der Waals interactions are the bonding mechanism between the encapsulated molecule and the tube.

1. Introduction

Nano-optoelectronics is the field in which the potential of single-walled carbon nanotubes (SWNTs) is greatest. However, despite the recent progress in nanoelectronics and photonic devices with SWNTs as active material,[1–3] such devices are limited to the near-infrared (NIR) region due to the intrinsically small bandgaps of SWNTs. Thanks to their particular size and geometry, the possibility to insert molecules as "peas" in the SWNT "pod" allows for them to be made optically active in the visible region. The encapsulation of molecules inside carbon nanotubes not only offers the opportunity of tuning the properties of the new hybrids but also keeps the peculiar physical properties of SWNTs.

After the first synthesis of organic "peapods" with encapsulated fullerenes (C_{60}) in carbon nanotubes,[4] the hollow space of these carbon cages attracted increasing interest. In the past decade, many materials, including metallofullerenes,

J. Gao, Prof. M. A. Loi
Zernike Institute for Advanced Materials
University of Groningen
Nijenborgh 4, Groningen, 9747 AG, The Netherlands
E-mail: M.A.Loi@rug.nl

Dr. P. Blondeau, Dr. P. Salice, Prof. E. Menna
ITM-CNR and Dipartimento di Scienze Chimiche
Università di Padova
Via Marzolo 1, 35131 Padova, Italy
E-mail: enzo.menna@unipd.it

DOI: 10.1002/smll.201100319

Dr. B. Bártová, Prof. C. Hébert
EPFL, SB-CIME & IPN-LSME
Bâtiment MXC, Station 12, 1015 Lausanne, Switzerland
E-mail: cecile.hebert@epfl.ch

J. Leschner, Prof. U. Kaiser
Central Facility of Electron Microscopy
Group of Materials Science
Albert-Einstein-Allee 11, 89081 Ulm, Germany

Dr. M. Milko, Prof. C. Ambrosch-Draxl,
Chair of Atomistic Modelling and Design of Materials
Montanuniversität Leoben, Franz-Josef-Straße 18, 8700 Leoben, Austria
E-mail: claudia.ambrosch-draxl@unileoben.ac.at

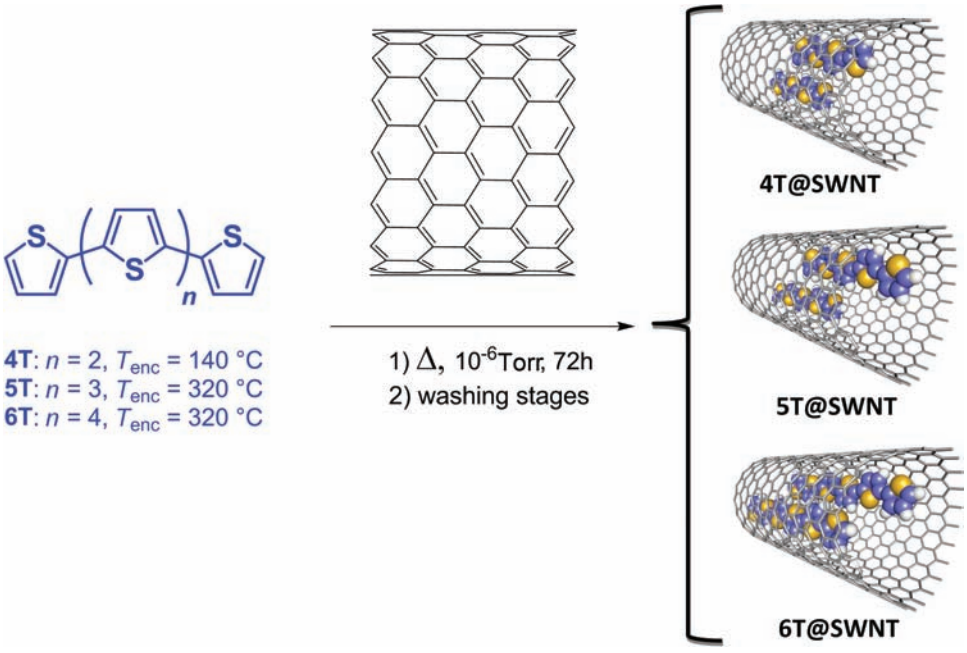

Figure 1. Scheme illustrating the encapsulation of α-quaterthiophene (4T), α-quinquethiophene (5T), and α-sexithiophene (6T) in SWNTs resulting in the corresponding peapods, labeled 4T@SWNT, 5T@SWNT, and 6T@SWNT. The carbon, hydrogen, and sulfur atoms of the oligothiophenes are represented in blue, white, and yellow, respectively. T_{enc} = encapsulation temperature.

metallocenes, organometallic molecules, and nanocrystals, have been successfully confined in the nanosized inner cavity of carbon nanotubes.[5–14] Up to now, however, only a few cases of filling SWNTs with complex organic molecules have been demonstrated.[15–21] Recently, the very first peapods with photoluminescence (PL) emission in the visible spectral range have been demonstrated by our team[22,23] by encapsulating α-sexithiophene (6T) inside SWNTs. α-Oligothiophenes are electron-rich and chemically stable conjugated oligomers, renowned for their superb optoelectronic properties and wide applications as active components in organic devices.[24–27] It is their linear conformation that makes them good candidates as guest molecules for peapod-like hybrids.

Herein, we present a study of the physical properties and electronic interactions in a series of peapods where thiophene oligomers, namely, α-quaterthiophene (4T), α-quinquethiophene (5T), and α-sexithiophene (6T), are encapsulated in SWNTs. The filling of the SWNTs is directly observed with aberration-corrected high-resolution transmission electron microscopy (AC-HRTEM) and further verified by Raman spectroscopy. Moreover, time-dependent AC-HRTEM images show the large mobility of the encapsulated molecules inside the SWNTs. As previously reported for the 6T peapod, the rest of the series also shows considerable PL quantum yields derived from the limited electronic interaction between the SWNTs and the oligothiophenes. Density functional theory (DFT) calculations confirm this finding and show how the electronic structure of the hybrid depends on the tube diameter and molecular length. It is shown that the interaction is purely van der Waals (vdW) like as the tube diameters are sufficiently large to perfectly accommodate the peas.

2. Results and Discussion

2.1. Synthesis of Peapods

Peapods were obtained by following a vapor-phase method based on the sublimation of the oligothiophenes in the presence of purified SWNTs in a sealed quartz tube at low pressure. The resulting adducts (4T@SWNT, 5T@SWNT, and 6T@SWNT, **Figure 1**) were separated from the nonencapsulated molecules by extensive washing with solvent and by treatment at reduced pressure to sublimate the molecules adsorbed on the external SWNT walls. The details of the reaction conditions and the washing procedure are presented in the Experimental Section.

2.2. AC-HRTEM

Figure 2 shows AC-HRTEM images of conjugated molecules inside the nanotube, namely 5T@SWNT. Since 6T-based peapods have already been investigated,[22] we concentrated on the 5T samples that turned out to be representative for all the sample series. Not only do the AC-HRTEM images reveal the successful encapsulation of the oligomers but also, as already found for 6T@SWNT,[22] they show two arrays of 5T molecules accommodated along the sidewalls of the tube. Time-dependent AC-HRTEM images show that the distance between the 5T molecules and the tube wall varies in the range of 0.26–0.39 nm over the period of observation. The 5T molecules bend and rotate inside the tube: during the observation the distance between the molecules along the direction perpendicular to the tube axis varies from

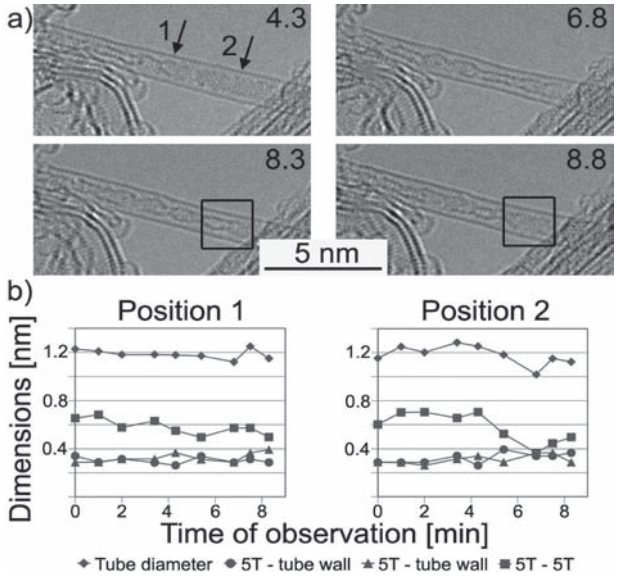

Figure 2. High-resolution images and molecular lengths. a) Measured TEM images of 5T@SWNT during different stages of observation. The time is given in minutes on the top right corner of the images. Black squares highlight different orientations of the 5T molecules inside the tube. b) Graphs showing the tube diameter, the distances between the 5T molecules and the tube wall, and the distance between two parallel molecular arrays during the time of observation. The measurements were performed at sites 1 and 2 marked by arrows in (a).

0.37 to 0.71 nm. A short movie showing the kinetics of the molecules inside the SWNTs can be seen in the Supporting Information.

The atomic model of a simple arrangement of two oligothiophene molecules inside a (16,0) SWNT with diameter 1.25 nm is depicted in **Figure 3**, together with an image simulation that was performed for straight 5T molecules either parallel or perpendicular to the electron beam. The simulated defocus maps from –6 to +6 nm in steps of 2 nm are shown in the bottom of Figure 3. Comparison of the simulations with Figure 2a does not allow for understanding unambiguously the orientation of the molecules in the snapshot taken at 4.3 min from the beginning of the observation.

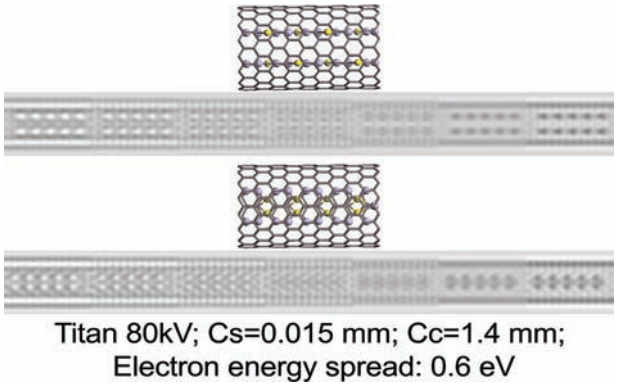

Figure 3. Atomic model of 5T molecules inside a (16,0) SWNT together with the corresponding simulation for the molecular plane parallel (left) and perpendicular (right) to the electron beam. The defocus varies from –6 to +6 in steps of 2 nm (from left to right).

The weak contrast observed could be assigned to both configurations. Later on, the molecules align in a configuration parallel to the electron beam and stronger contrast can be seen, although it is clear from the measured images that the molecules are bent. At the end of the observation (after 8.8 min), the contrast gets weaker again in one part of the SWNT. We conclude that a relatively long time (≈10 min) of observation at 80 kV has no destructive effect on the peapod, and that the encapsulated molecule is rotating inside the SWNT.

2.3. Raman Spectroscopy

Raman spectroscopy is one of the most useful techniques to demonstrate the encapsulation of molecules inside SWNTs. In **Figure 4**, the Raman spectra measured for all peapods and control samples excited at a 488 nm laser line are reported. At this excitation wavelength, the control experiment is particularly valuable since the oligothiophene Raman spectrum could not be measured due to the strong PL. Additional measurements were performed with a 633 nm laser excitation. The corresponding results are shown in the Supporting Information (Figure 1). After encapsulation, the radial breathing mode (RBM) bands of the SWNT are upshifted, as shown in Figure 4b,e,h. Such behavior is not observed for the control experiments in which the SWNTs and the oligomers are mixed. This change can be ascribed to hardening and stiffening of C–C bonds and it is in good agreement with previously reported characterizations of fullerene-based peapod materials.[21,28] Indeed, the variation in frequency of the RBM is symptomatic of the inclusion of entities in the hollow space of the SWNTs. The technique also allows estimation of the filling ratio of the SWNTs with different oligomers by looking at the intensity of the molecular vibrations. From this analysis the highest filling ratio is obtained for 6T while the filling for the 4T is poor. However, it is important to underline that only qualitative data can be obtained in this way because of the different resonance conditions for the different oligomers.

Raman spectroscopy also allows investigation of the interaction mechanism between the molecules and SWNTs. In this study, excitation with a 488 nm laser line is resonant with the absorption of the 6T peapod. Charge transfer from the excited state of the molecule to the SWNT, if present, should result in the presence of radical cations of 6T ($6T^+$). This cation has been studied by Raman spectroscopy and was shown to give rise to a large downshift from 1459 to 1440 cm^{-1},[29] which was not observed in the Raman spectra of our peapods. Moreover, charge transfer between a molecule and SWNTs always results in a shift of the G-band and an RBM intensity reduction.[19] Again, such effects were not observed, which evidences that charge transfer does not occur in this peapod.[30] In addition, a new and symptomatic peak is detected at 1504, 1501, and 1499 cm^{-1} for 4T, 5T, and 6T peapods, respectively. Assuming that encapsulated oligothiophene molecules are not charged, the intermolecular interaction and the constraint from the tube wall account for these spectral shifts.

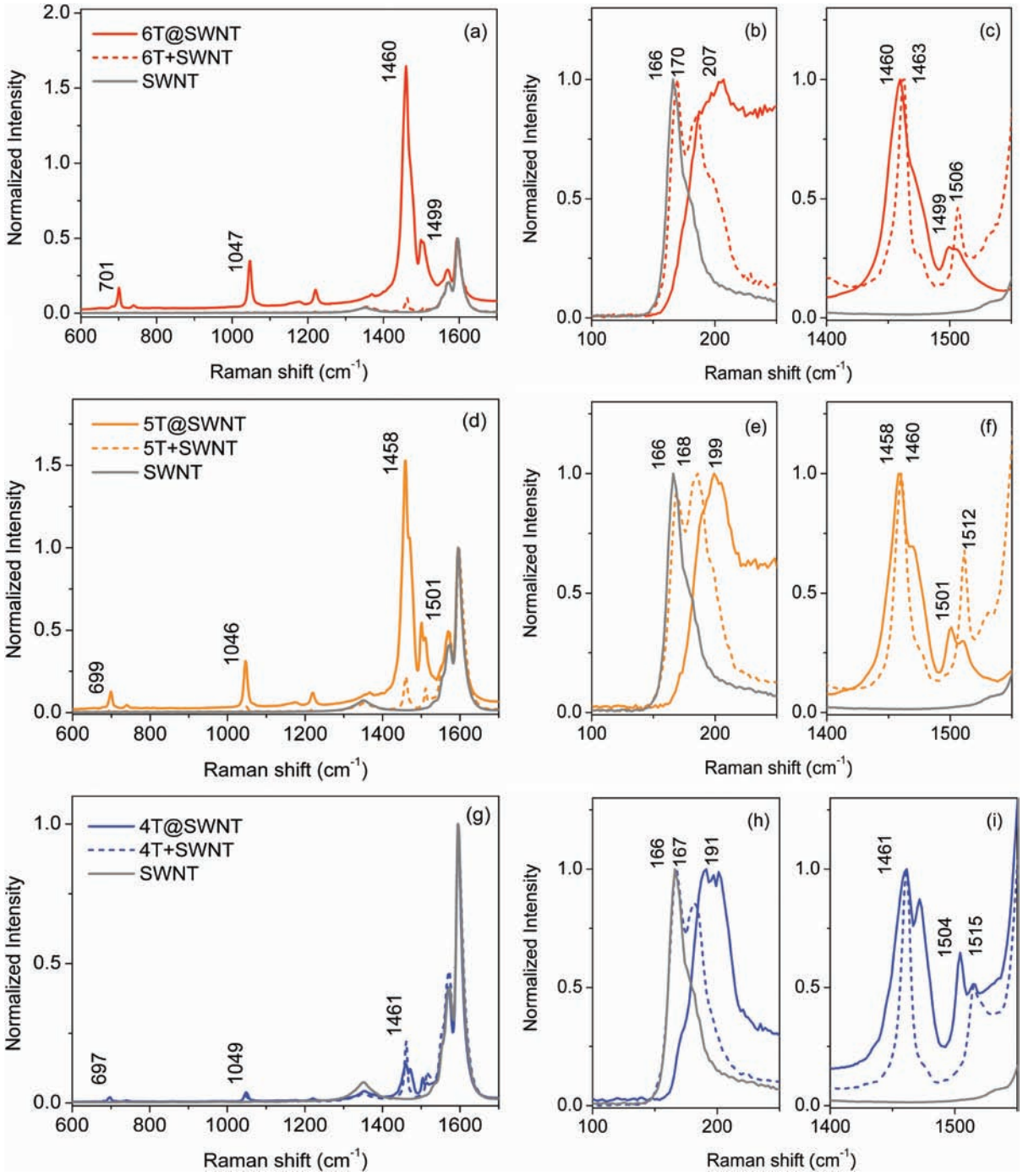

Figure 4. Raman spectra: 600–1700 nm spectral region (a), radial breathing mode (RBM) (b), and C C stretching modes (c) of 6T@SWNT (red), control sample (mixture of molecule and SWNTs, dashed red), and pure SWNTs (gray). d–f) Same as (a)–(c) but for 5T (orange curves). g–i) Same as (a)–(c) but for 4T (blue curves). The excitation wavelength was set at 488 nm. All spectra are normalized at their maximum peak frequencies.

2.4. Photophysics of Peapods

In view of the possibility of using peapods as active material for optoelectronic devices, the investigation of the optical properties of the nanohybrids is crucial. **Figure 5** depicts the photophysics of the three peapods. Visible PL emission from the encapsulated molecules is observed in all the samples. It is important to underline that all the peapods have been extensively washed from the conjugated molecules adsorbed on the external walls. The effectiveness of the washing procedure (>12 h vacuum washing) is proven by the negligible PL emission of the washing solution (Supporting Information, Figure 2), which testifies that the visible emission originates from the encapsulated molecules. Figure 5a, c, and e show the PL excitation spectra of the peapods together with the corresponding molecules in diluted solution. The detection wavelength was set at 550, 520, and 490 nm for 6T, 5T, and 4T peapods, respectively. All the excitation spectra show that

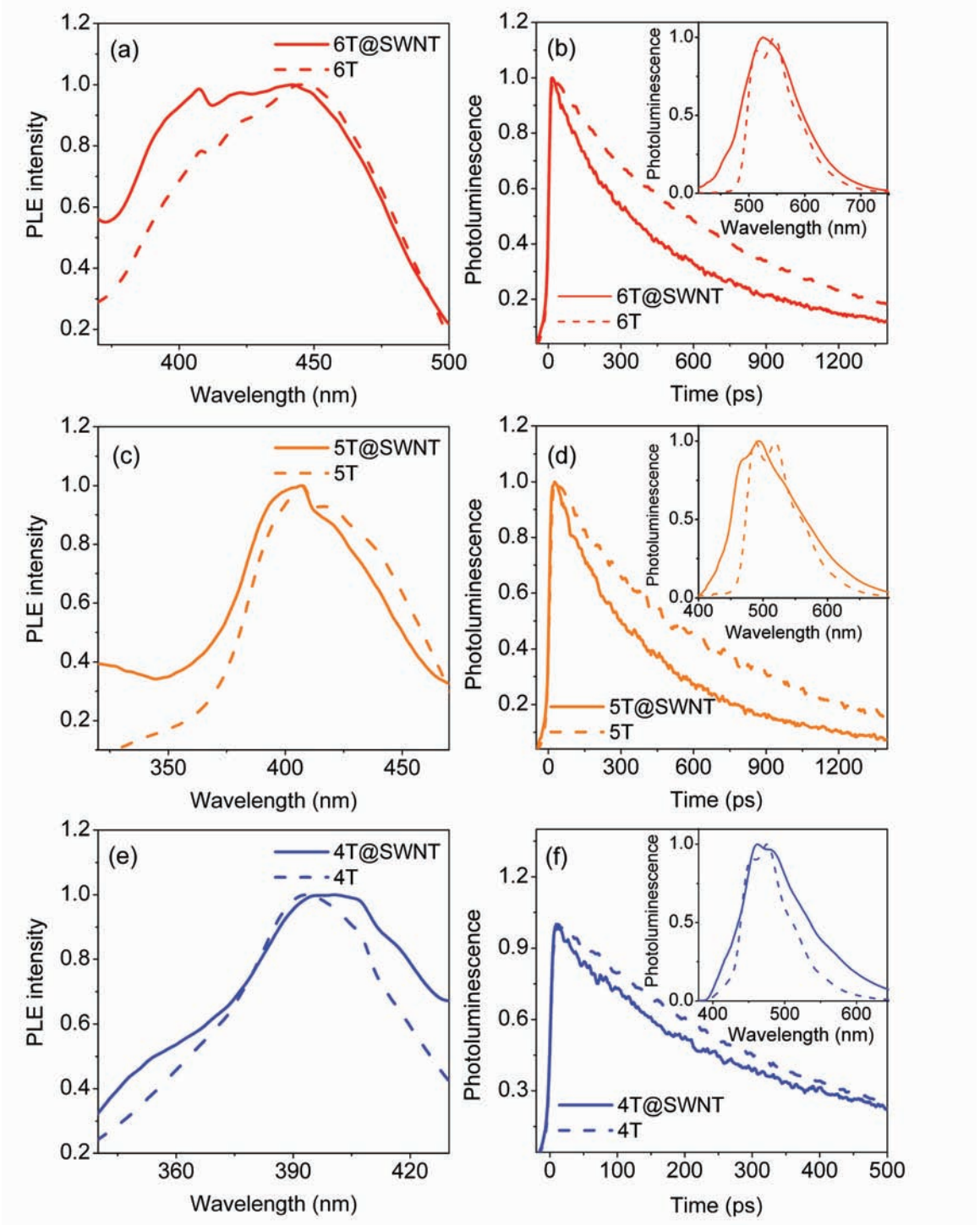

Figure 5. Photoluminescence excitation (PLE) spectra of 6T@SWNT and 6T (a), 5T@SWNT and 5T (c), and 4T@SWNT and 4T (e). PL decays of 6T@SWNT and 6T (b), 5T@SWNT and 5T (d), and 4T@SWNT and 4T (f). Insets show the corresponding PL spectra.

while the main features of the solution and peapod spectra are superimposed, the high-energy region of the peapod spectrum is always more pronounced. Such differences most probably indicate either mixing of high-energy states or energy transfer to the encapsulated molecules. The insets of Figure 5b, d, and f show the PL spectra of the peapods and of the isolated molecules. The peapods always exhibit less-resolved features compared to those of the molecules. There are several possible explanations for such variation. First, the dielectric constant of the solvent for oligothiophene molecules in solution ($\varepsilon_{solvent} \approx 38$) is much larger than that of the microenvironment of the encapsulated molecules ($\varepsilon_{carbon} \approx 3$). Second, the interaction of the molecules with the SWNT walls or between neighboring molecules in this highly confined system could also have an impact on the PL spectra. The optical properties of oligothiophenes, particularly 6T,

are very sensitive to their supermolecular interaction,[31,32] and different physical dimers can lead to large differences in the absorption and PL spectra.[33] However, the differences between the PL spectra of our peapods and those of the corresponding molecules cannot be interpreted in terms of dimer formation. This supports the assumption that the overall optical properties are more influenced by the interaction between the encapsulated molecules and the SWNT walls than by intermolecular interactions. This finding is also in agreement with the AC-HRTEM measurements, thus proving that the encapsulated molecules show increased spatial affinity to the sidewall instead of to other molecules.

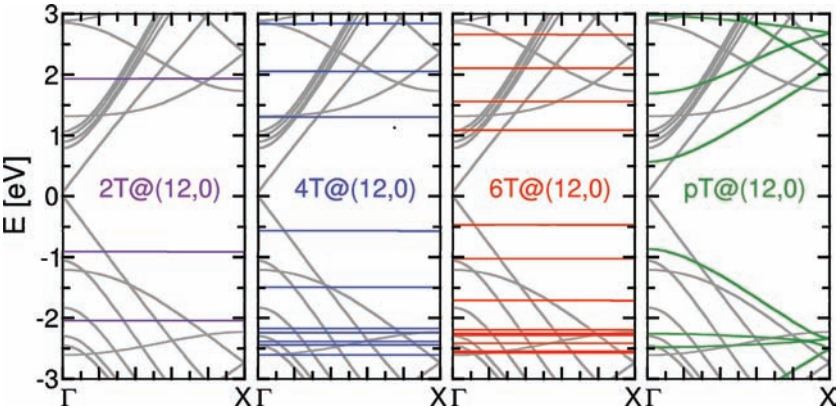

Figure 6. Band structure of peapods consisting of a (12,0) SWNT with (left to right) encapsulated 2T, 4T, 6T, and pT, respectively. The gray lines indicate the bands originating from the tube, while the colored lines mark the levels arising from the molecule or polymer.

The results of time-resolved PL measurements are shown in Figure 5b,d,f. The PL lifetimes of the encapsulated molecules are always shorter than those of the isolated ones [563 (6T@SWNT) versus 813 ps (6T), 389 (5T@SWNT) versus 695 ps (5T), and 265 (4T@SWNT) versus 370 ps (4T)]. However, the reduction of the lifetime is limited to 30% of the intrinsic value, which indicates a rather efficient emission from the peapods. By considering the quantum yields (QYs) of the molecules in solution,[34] it is possible to estimate the QY of the peapods to be 12.9% for 4T@SWNT, 19% for 5T@SWNT, and 30.5% for 6T@SWNT.

The PL quenching of the encapsulated molecules can be rationalized by the interaction with the SWNT cage. The PL lifetime of isolated semiconducting SWNTs is around tens of picoseconds and dominated by nonradiative processes.[35] In SWNT bundles, the PL decay of semiconducting species is reported to be much faster due to energy transfer to those with smaller bandgaps and to the screening by metallic nanotubes.[36,37] SWNTs used for the peapod synthesis are composed of both semiconducting and metallic nanotubes, which can provide additional pathways for nonradiative emission of the encapsulated molecules. The occurrence of energy transfer from the molecules to SWNTs can neither be excluded nor unambiguously proven at this stage.

The efficient light emission from encapsulated molecules inside SWNTs demonstrates remarkable potential for future material design. Similarly, emission from the inner tube of double-walled carbon nanotubes (DWNTs) has been reported. The photophysical properties of the inner tube, such as PL spectra and/or fluorescence lifetime, were observed to be modified due to the interaction with the external tube.[38,39]

2.5. Electronic Structure

The Kohn–Sham band structures of the hybrid systems with different thiophene oligomers as peas are depicted in **Figure 6**, and demonstrate the dependence on the molecular length. The electronic states stemming from 2T, 4T, 6T, and polythiophene (pT) are highlighted in violet, blue, red, and green, respectively, while gray lines represent the bands originating from the (12,0) SWNT. These electronic tubelike levels, which were calculated in different supercell geometries, are back-folded to the elementary unit cell to allow for comparison. The growing number of thiophene rings results in an increase of molecular states in the considered energy range and, consequently, a decreased HOMO–LUMO splitting. This finally gives rise to the band dispersion for the limiting case of the polymer (Figure 6, left).

We note here again that in our calculations, the C–C bond connecting the individual rings of the pT was stretched in order to achieve a commensurate unit cell with the tube. Therefore, although the bandgap of 6T is already close to that of pT, the level alignment deviates from the general trend.

This system, nevertheless, allows for studying the effect of encapsulation on the electronic properties. In **Figure 7**, we focus on the geometric arrangement of pea and pod, by depicting the electronic structures of peapods (green dots) with pT embedded in a (10,0) and a (16,0) SWNT (left and middle), while in the right panel two polymer chains are accommodated in the (16,0) nanotube. In addition, the bands of the corresponding nanotubes are shown as gray lines. PT encapsulated in the (10,0) SWNT represents an example where the tube diameter is too small to accommodate the guest. This results not only in a positive binding energy,[22] but also in structural distortions as seen in the inset. In such cases, there is also considerable charge transfer between the two subsystems. Consequently, the electronic bands of the combined system originating from the SWNT do not coincide with those of the pure SWNT (gray lines). In contrast, for larger tubes, such as those depicted in the middle and right-hand panels, this is perfectly the case. Here, the peapod bands arising from the tube are basically identical to those of the pristine tubes, and the interaction between pea and pod is merely vdW like.

There are two small differences between a singly and a doubly occupied peapod. The first is a band splitting of 0.06 eV arising from a very weak interchain interaction. Its magnitude only slightly depends on the particular cofacial arrangement of the chains. Figure 7 depicts the results for the case where these are shifted with respect to each other by half

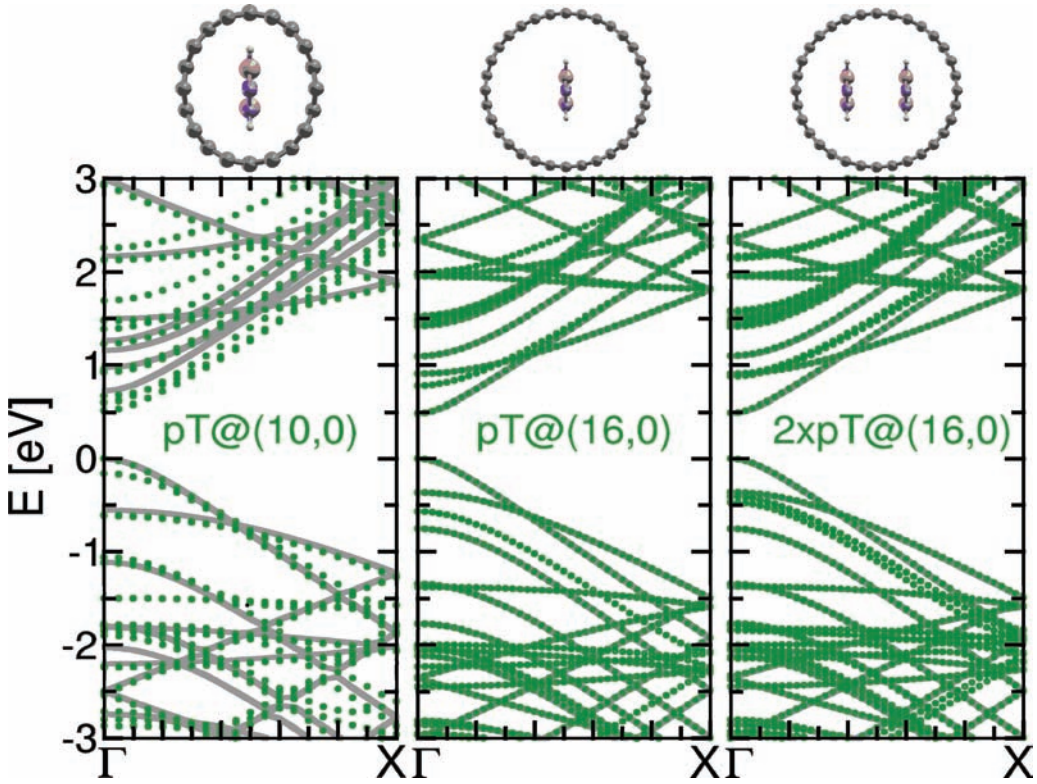

Figure 7. Band structures of pT (green dots) embedded in a (10,0) (left) and (16,0) SWNT (middle). The right panel depicts the results for two pT chains encapsulated in a (16,0) tube. For comparison, the bands of the pristine SWNTs are indicated by gray lines.

a thiophene ring. The second difference is seen in the band alignment. Compared to the SWNT with one pT chain inside, the polymer bands are here found to be somewhat higher in energy.

Generally, one can conclude that the electronic structure of oligothiophene peapods highlights the weak vdW-like bonding between the two pristine systems. In all energetically stable cases we have studied, we find that the electronic states stemming from different subunits of the peapod change neither dispersion nor bandgap. In fact, the band structure of the combined system always appears like a mere superposition of the respective constituents' bands. (The mechanism behind the alignment is discussed elsewhere.[40]) This situation impressively supports the findings from Raman spectroscopy that basically no charge transfer occurs between pea and pod.

3. Conclusion

In summary, we have synthesized and fully characterized nanohybrids with tunable electronic structure and emission in the visible range by the encapsulation of a series of oligothiophenes in SWNTs. Visible PL can be observed from all the peapods with QYs up to 30%. The configuration and kinetics of the encapsulated molecules inside the SWNTs are demonstrated by AC-HRTEM, which shows two arrays of molecules parallel to the SWNT walls. DFT calculations demonstrate vdW interaction as the bonding mechanism between the tube and the encapsulated molecule. This is reflected in the electronic structure as well as in the measured Raman spectra. Only for small tubes is a considerable tube distortion and charge transfer predicted. Interaction between pea and pod seems to exist, however, in the excited state as evidenced by optical measurements. The hybrids investigated here exhibit exciting properties which could fulfill many demands for the design of nanomaterials and, hence, are expected to play a role in future nanophotonic device applications.

4. Experimental Section

Sample Preparation Instruments: For low-power sonications a 150-W ultrasonic cleaning bath, operating at 45 kHz, was used, while for high-power sonications a 600-W ultrasonic processor equipped with a titanium microtip was employed. An IEC CL10 centrifuge (Thermo Electron Corporation) was utilized for all procedures.

Purification of SWNTs: SWNTs purchased from NanoCarblab (SWNT purity: 70–80 wt%, diameter: 1.2–1.4 nm, length: 1–5 m, batch NCL K68) were heated at 1100 C under 10^{-6} Torr to remove the carboxylic groups that could prevent the encapsulation of molecules. In detail, SWNTs (80 mg) were placed in a quartz tube (inside diameter I.D. = 5 mm, length L = 150 mm), which was brought to 10^{-6} Torr and sealed. The quartz tube was heated at 1100 C for 1 h and then allowed to reach room temperature slowly.

Encapsulation of Oligothiophenes: Oligothiophenes were purchased from Tokyo Chemical Industry (TCI). Purification of 2,2′:5′,2″:5″,2‴-quaterthiophene (4T) was achieved according to Papagni et al.[41] To this extent, 4T (30 mg) was purified by column

chromatography with silica gel activated coal (20:1, 10 g) as stationary phase and toluene as eluent. The yellow residue obtained after removing the solvent at reduced pressure was sublimated at 0.05 Torr and 140 C affording a pure sample of 4T.

Purified 4T (6.1 mg) and annealed SWNTs (5.3 mg) were suspended in chloroform (0.5 mL) and placed in a quartz tube (I.D. = 5 mm, L = 150 mm). The solvent was removed by heating and the quartz tube was brought to 10^{-7} Torr, sealed 50 mm from the bottom, and then heated at 140 C for 72 h. The carbonaceous material was recovered by opening the quartz tube, and the excess of 4T was removed in three stages:

1) Solvent washing (20 × 7 mL toluene, high-power sonication, and then centrifugation);
2) Dynamic vacuum washing (heating the sample for 8 h at 200 C and 10^{-2} Torr) followed by a solvent washing stage (18 × 7 mL toluene, high-power sonication, and then centrifugation);
3) Dynamic vacuum washing (heating the sample for 16 h at 200 C and 10^{-2} Torr) followed by a solvent washing stage (10 × 7 mL toluene, pulsed sonication, and then centrifugation).

The washing procedure was thoroughly followed by subjecting the washing solutions to fluorescence analysis (see Supporting Information). We will henceforth refer to the black powder obtained after the third washing stage as 4T@SWNT.

2,2′:5′,2″:5″,2‴:5‴,2⁗-Quinquethiophene (5T) and 2,2′:5′,2″:5″,2‴:5‴,2⁗:5⁗,2⁗′-sexithiophene (6T) were purchased from TCI and were treated according to the above-mentioned procedure to obtain peapods labeled 5T@SWNT and 6T@SWNT, respectively.

The control experiment was performed through the following procedure: SWNTs (1 mg) in CH_2Cl_2 (1 mL) were sonicated for 10 min, then dried under N_2 flow; oligothiophene (0.1 mg) in CH_2Cl_2 (1 mL) was added to the SWNTs and quickly dried under N_2 flow to avoid any encapsulation of the single molecules. The resulting solid samples are referred to as 4T+SWNT, 5T+SWNT, and 6T+SWNT.

AC-HRTEM: For the HRTEM measurements a suspension of peapods in toluene was sonicated for 10 min and dropped onto a holey carbon grid. An FEI Titan 80–300 high-resolution transmission electron microscope equipped with a CEOS-designed hexapole-based aberration corrector for the image-forming lens was operated at 80 kV. This way, the electron knock-on damage to the sample was reduced. The specimen was kept at room temperature during the experiment. A Gatan MSC794 (1k × 1k, 14 bit) CCD camera was used for digital recording of HRTEM pictures. The spherical aberration was adjusted to $C_s \approx +15$ m and a set of HRTEM images was recorded with a 2-s delay. A short movie was made from a set of images that were drift-corrected using ImageJ software.[42] We present the images in slightly underfocused conditions to enhance the contrast of the molecule inside the SWNT. The HRTEM image simulations were performed with a standard multislice procedure.[43]

Theory: All calculations were performed in the framework of DFT utilizing the planewave code Quantum Espresso.[44] A supercell approach was adopted, in which the repeat unit of the SWNT was doubled to accommodate polythiophene (pT) inside. To ensure commensurability of the polymer with the SWNT, the former had to be stretched by 8%. For embedding bithiophene (2T), 4T, and 6T, the unit cell size had to be taken as three, five, and seven times the length of the SWNT, respectively. A vacuum size of 8 Å in the perpendicular direction turned out large enough to prevent interactions of neighboring tubes. The generalized gradient approximation (GGA) was employed, and 4 k points in the irreducible wedge of the Brillouin zone (BZ) were used for the self-consistent field (SCF) calculations. In a first step, the pristine structures were relaxed independently. The geometries were considered to be relaxed when all atomic forces were smaller than 1 mRy $Å^{-1}$. These geometries served as a starting point for the investigations of the combined systems that were then optimized including vdW interactions treated in an ab initio post-SCF manner.[45,46]

Optical Spectroscopy: UV/vis–NIR spectra were recorded with a Cary 5 Varian spectrometer. Raman spectra were obtained with an Invia Renishaw Raman microspectrometer (50× objective) equipped with 488 and 633 nm laser sources. The measurements were carried out with the samples on KBr pellets. PL excitation spectra were recorded with a Perkin–Elmer LS 50B spectrometer. For time-resolved and steady-state PL measurements, the solutions were excited by a 150-fs-pulsed Kerr-mode-locked Ti:sapphire laser, frequency doubled at about 380 nm and the steady-state PL emission was measured with CCD detector. The time-resolved PL was recorded by a Hamamatsu streak camera working in synchroscan mode. The decays were fitted using a single exponential decay function. All measurements were performed at room temperature and the spectra were calibrated for the instrumental response.

Supporting Information

Supporting Information is available from the Wiley Online Library or from the author.

Acknowledgements

This work was carried out within the framework of NanoSci-ERA (a consortium of national funding organizations within the European Research Area), project Nano-Hybrids for Photonic Devices (NaPhoD). M.A.L. and J.G. acknowledge the financial support of Technologiestichting STW. C.A.-D. and C.H. appreciate funding from the Austrian Science Fund, projects I107 and I108. E.M. wishes to thank MIUR (contracts RBFR08DUX6 and 20085M27SS) and the University of Padova ("Progetto Strategico" HELIOS, prot. STPD08RCX) for funding. E.M., P.B., and P.S. thank Prof. Moreno Meneghetti for helpful discussions.

[1] J. A. Misewich, R. Martel, Ph. Avouris, J. C. Tsang, S. Heinze, J. Tersoff, *Science* **2003**, *300*, 783.
[2] J. Chen, V. Perebeinos, M. Freitag, J. Tsang, Q. Fu, J. Liu, Ph. Avouris, *Science* **2005**, *310*, 1171.
[3] Ph. Avouris, M. Freitag, V. Perebeinos, *Nat. Photonics* **2008**, *2*, 341.
[4] B. W. Smith, M. Monthioux, D. E. Luzzi, *Nature* **1998**, *396*, 323.
[5] L. J. Li, A. N. Khlobystov, J. G. Wiltshire, G. A. D. Briggs, R. J. Nicholas, *Nat. Mater.* **2005**, *4*, 481.
[6] R. Kitaura, H. Shinohara, *Chem. Asian J.* **2006**, *1*, 646.
[7] J. Lu, S. Nagase, D. Yu, H. Ye, R. Han, Z. Gao, S. Zhang, L. Peng, *Phys. Rev. Lett.* **2004**, *93*, 116804.

[8] A. N. Khlobystov, D. A. Britz, G. A. D. Briggs, *Acc. Chem. Res.* **2005**, *38*, 901.
[9] Y. Iizumi, T. Okazaki, Z. Liu, K. Suenaga, T. Nakanishi, S. Iijima, G. Rotas, N. Tagmatarchis, *Chem. Commun* **2010**, *46*, 1293.
[10] Y. Ren, G. Pastorin, *Adv. Mater.* **2008**, *20*, 2031.
[11] J. Sloan, A. I. Kirkland, J. L. Hutchison, M. L. H. Green, *Acc. Chem. Res.* **2002**, *35*, 1054.
[12] J. G. Wang, Y. A. Lv, X. N. Li, M. D. Dong, *J. Phys. Chem. C* **2009**, *113*, 890.
[13] J.-P. Tessonnier, O. Ersen, G. Weinberg, C. Pham-Huu, D. S. Su, R. Schlogl, *ACS Nano* **2009**, *3*, 2081.
[14] a) P. M. F. J. Costa, D. Golberg, M. Mitome, S. Hampel, A. Leonhardt, B. Buchner, Y. Bando, *Nano Lett.* **2008**, *8*, 3120; b) A. Chuvilin, A. N. Khlobystov, D. Obergfell, M. Haluska, S. Yang, S. Roth, U. Kaiser, *Angew. Chem. Int. Ed.* **2010**, *49*, 193.
[15] a) K. Yanagi, K. Iakoubovskii, H. Matsui, H. Matsuzaki, H. Okamoto, Y. Miyata, Y. Maniwa, S. Kazaoui, N. Minami, H. Kataura, *J. Am. Chem. Soc.* **2007**, *129*, 4992; b) N. Tschirner, K. Brose, J. Maultzsch, K. Yanagi, H. Kataura, C. Thomsen, *Phys. Status Solidi B* **2010**, *247*, 2734.
[16] K. Yanagi, K. Iakoubovskii, S. Kazaoui, N. Minami, Y. Maniwa, Y. Miyata, H. Kataura, *Phys. Rev. B* **2006**, *74*, 155420.
[17] K. Yanagi, Y. Miyata, Z. Liu, K. Suenaga, S. Okada, H. Kataura, *J. Phys. Chem. C* **2010**, *114*, 2524.
[18] S. Campestrini, C. Corvaja, M. De Nardi, C. Ducati, L. Franco, M. Maggini, M. Meneghetti, E. Menna, G. Ruaro, *Small* **2008**, *4*, 350.
[19] T. Takenobu, T. Takano, M. Shiraishi, Y. Murakami, M. Ata, H. Kataura, Y. Achiba, Y. Iwasa, *Nat. Mater.* **2003**, *2*, 683.
[20] Y. Fujita, S. Bandow, S. Iijima, *Chem. Phys. Lett.* **2005**, *413*, 410.
[21] a) H. Kataura, Y. Maniwa, M. Abe, A. Fujiwara, T. Kodama, K. Kikuchi, H. Imahori, Y. Misaki, S. Suzuki, Y. Achiba, *Appl. Phys. A: Mater. Sci. Process.* **2002**, *74*, 349; b) M. C. Gimenez-Lopez, A. Chuvilin, U. Kaiser, A. N. Khlobystov, *Chem. Commun.* **2011**, *47*, 2116.
[22] M. A. Loi, J. Gao, F. Cordella, P. Blondeau, E. Menna, B. Bártová, C. Hébert, S. Lazar, G. A. Botton, M. Milko, C. Ambrosch-Draxl, *Adv. Mater.* **2010**, *22*, 1635.
[23] K. Yanagi, H. Kataura, *Nat. Photonics* **2010**, *4*, 200.
[24] A. R. Murphy, J. M. J. Fréchet, *Chem. Rev.* **2007**, *107*, 1066.
[25] M. K. R. Fischer, S. Wenger, M. Wang, A. Mishra, S. M. Zakeeruddin, M. Grätzel, P. Bäuerle, *Chem. Mater.* **2010**, *22*, 1836.
[26] M.-Y. Yoon, S. A. DiBenedetto, M. T. Russell, A. Facchetti, T. J. Marks, *Chem. Mater.* **2007**, *19*, 4864.
[27] F. Dinelli, R. Capelli, M. A. Loi, M. Murgia, M. Muccini, A. Facchetti, T. J. Marks, *Adv. Mater.* **2006**, *18*, 1416.
[28] D. A. Britz, A. N. Khlobystov, *Chem. Soc. Rev.* **2006**, *35*, 637.
[29] N. Yokonuma, Y. Furukawa, M. Tasumi, M. Kuroda, J. Nakayama, *Chem. Phys. Lett.* **1996**, *255*, 431.
[30] M. Kalbáč, L. Kavan, S. Gorantla, T. Gemming, L. Dunsch, *Chem. Eur. J.* **2010**, *16*, 11753.
[31] E. Da Como, M. A. Loi, M. Murgia, R. Zamboni, M. Muccini, *J. Am. Chem. Soc.* **2006**, *128*, 4277.
[32] M. A. Loi, E. Dacomo, F. Dinelli, M. Murgia, R. Zamboni, F. Biscarini, M. Muccini, *Nat. Mater.* **2005**, *4*, 81.
[33] M. Pope, *Electronic Processes in Organic Crystals and Polymers*, Oxford University Press, Oxford, UK **1999**.
[34] R. S. Becker, J. S. deMelo, A. L. Macanita, F. Elisei, *J. Phys. Chem.* **1996**, *100*, 18683.
[35] Y. Homma, S. Chiashi, Y. Kobayashi, *Rep. Prog. Phys.* **2009**, *72*, 066502.
[36] J.-S. Lauret, C. Voisin, G. Cassabois, C. Delalande, Ph. Roussignol, O. Jost, L. Capes, *Phys. Rev. Lett.* **2003**, *90*, 057404.
[37] a) J. Gao, M. Kwak, J. Wildeman, A. Herrmann, M. A. Loi, *Carbon* **2011**, *49*, 333; b) J. Gao, M. A. Loi, *Eur. Phys. J. B* **2010**, *75*, 121.
[38] T. Hertel, A. Hagen, V. Talalaev, K. Arnold, F. Hennrich, M. Kappes, S. Rosenthal, J. McBride, H. Ulbricht, E. Flahaut, *Nano Lett.* **2005**, *5*, 511.
[39] H. Muramatsu, T. Hayashi, Y. A. Kim, D. Shimamoto, M. Endo, V. Meunier, B. G. Sumpter, M. Terrones, M. S. Dresselhaus, *Small* **2009**, *5*, 2678.
[40] M. Milko, P. Puschnig, C. Ambrosch-Draxl, unpublished.
[41] S. Trabattoni, S. Laera, R. Mena, A. Papagni, A. Sassella, *J. Mater. Chem.* **2004**, *14*, 171.
[42] W. S. Rasband, ImageJ, US National Institutes of Health, BethesdaMaryland, http://rsb.info.nih.gov/ij/, 1997–2009.
[43] P. A. Stadelmann, JEMS, http://cimewww.epfl.ch/people/stadelmann/jemsWebSite/jems.html, EPFL, Lausanne, last accessed: February 2011.
[44] P. Giannozzi, S. Baroni, N. Bonini, M. Calandra, R. Car, C. Cavazzoni, D. Ceresoli, G. L. Chiarotti, M. Cococcioni, I. Dabo, A. D. Corso, S. de Gironcoli, S. Fabris, G. Fratesi, R. Gebauer, U. Gerstmann, C. Gougoussis, A. Kokalj, M. Lazzeri, L. Martin-Samos, N. Marzari, F. Mauri, R. Mazzarello, S. Paolini, A. Pasquarello, L. Paulatto, C. Sbraccia, S. Scandolo, G. Sclauzero, A. P. Seitsonen, A. Smogunov, P. Umari, R. M. Wentzcovitch, *J. Phys.: Condens. Matter.* **2009**, *21*, 395502.
[45] M. Dion, H. Rydberg, E. Schröder, D. C. Langreth, B. I. Lundqvist, *Phys. Rev. Lett.* **2004**, *92*, 246401.
[46] D. Nabok, P. Puschnig, C. Ambrosch-Draxl, *Phys. Rev. B* **2008**, *77*, 245316.

Received: February 12, 2011
Revised: March 16, 2011
Published online: